

Full Length Research Paper

Characterization and optimization of poly (3-hexylthiophene-2, 5- diyl) (P3HT) and [6, 6] phenyl-C₆₁-butyric acid methyl ester (PCBM) blends for optical absorption

G. Kalonga^{1*}, G. K. Chinyama², M. O. Munyati³ and M. Maaza⁴

¹Department of Physics, School of Natural Sciences, University of Zambia, P. O. Box 32379, Lusaka, 10101 Zambia.

²Department of Physical Sciences, School of Mathematics and Natural Sciences, The Copperbelt University, P.O. Box 21692, Kitwe, Zambia.

³Department of Chemistry, School of Natural Sciences, University of Zambia, P. O. Box 32379, Lusaka, 10101 Zambia.

⁴Nanosciences Laboratories, Materials Research Department, iThemba LABS, P. O. Box 722, Somerset West 7129, Western Cape, South Africa.

Accepted 19 August, 2013

Thin films were developed, characterized, and optimized for optical absorbance from blends of organic polymer poly (3-hexylthiophene-2, 5- diyl) (P3HT) and the fullerene derivative [6, 6] phenyl-C₆₁-butyric acid methyl ester (PCBM). The materials of both pristine and blends were analyzed using X-ray diffraction spectroscopy and high resolution transmission electron microscopy for structural properties, and fourier transform infra-red and UV-VIS spectroscopy for optical properties. The study evaluated the effects of altering the blend ratio and annealing temperature on absorption. The ratios were made by varying the weight of PCBM whilst keeping that of P3HT constant. Eleven different ratios were made with each exhibiting its own optimal annealing temperature and absorption. The optimum ratio was determined and found to be at 1:1 with an annealing temperature of 100°C for 30 min duration.

Key words: Poly (3-hexylthiophene-2, 5- diyl) (P3HT), [6, 6] phenyl-C₆₁-butyric acid methyl ester (PCBM), blend ratio, thin films, organic, polymer.

INTRODUCTION

Semi-conducting organic polymers play a crucial role towards the possible realization of commercial solar energy absorbers that are flexible and light in weight (Ma et al., 2005; Shaheen et al., 2001; Chirvase et al., 2004; Usami, 2000). Among the promising polymers in this category is poly (3-hexylthiophene-2, 5- diyl) also known as P3HT. P3HT is a conjugated polymer with a band gap of 2.1 eV and lowest unoccupied molecular orbital (LUMO) levels at 2.7 eV. It acts as an electron donor during the photo-excitation process and exhibits a high

hole mobility in the range of $10^{-3} \text{ cm}^2 \text{ V}^{-1} \text{ s}^{-1}$ in poorly organized thin films to $2 \times 10^{-1} \text{ cm}^2 \text{ V}^{-1} \text{ s}^{-1}$ in well crystallized films (Chirvase et al., 2004; Koster, 2007; Muhlbacher et al., 2006; Woehrle and Meissner, 1991). The optical absorption peak of pristine P3HT is at about 550 nm wavelength, a region rich in energy in relation to the solar spectrum at 1.5 AM (Shockley and Queisser, 1961).

Despite P3HT having good hole mobility, its performance in photovoltaic application as a standalone

conductor is limited due to the fact that charge carriers are still bound up in form of excitons. To improve its role in photovoltaic applications, another interfacing material that will enable exciton dissociation to take place is required. The interfacing material should also act as an electron acceptor and must be a matching candidate to provide the offset potential required for the exciton dissociation to occur leading to generation of free charge carriers at the interface between the two (Chirvase et al., 2004; Shockley and Queisser, 1961; Brabec et al., 2001; Green, 1982; Adam et al., 1993). A promising electron acceptor candidate for P3HT is [6, 6] phenyl-C₆₁-butyric acid methyl ester also known as C₆₀-PCBM or simply PCBM (Hoppe et al., 2005; Gartstein and Conwel, 1995; Lane et al., 2000; Nguyen et al., 2007). PCBM is a small molecule fullerene derivative with a band gap of 2.3 eV and LUMO levels at 3.8 eV with an absorption peak in the ultraviolet region (Koster, 2007). The electron mobility of PCBM is relatively low and is reported to be between 2×10^{-3} and 2×10^{-2} cm² V⁻¹ s⁻¹ and has been cited as the major drawback for PCBM's applications in various photo-devices such as solar cells and photo-diodes (Muhlbacher et al., 2006). However, blending the two materials produces new electrical and absorption properties, and it is anticipated that it can produce relatively high efficient and yet cheap and flexible photo-devices compared to that of pure P3HT. In this study, blending was used as a means of interfacing the two materials at a molecular level.

In order to fully understand the underlying principles and realize the full potential of such a system, key parameters such as blend ratio and annealing temperatures need to be characterized and optimized. In this report, therefore, thin films were developed from the blend of P3HT and PCBM to form a thin film blend system (Dunlap et al., 1996; Sze, 1981 Friend et al., 1997). To determine the optimum blend ratio, different ratios by weight of the two materials were studied. Previous studies by different scholars on the blend ratios randomly looked at a wide number of weight ratios such as 1:3, 1:2, 1:1.5, 1:1, 1:0.9, 1:0.8, and 1:0.7. Results from these studies point out that the optimum blend ratio is between 1:0.9 and 1:1, but fail short of specifying the exact optimal ratio (Woehrlé and Meissner, 1991). Some other studies however have made mention of 1:1 as the optimal ratio while others have mentioned 1:0.80 or 1:0.43 (Camaioni et al., 2002; Dennler et al., 2009; Chen et al., 2009). This study specifically focuses on the blend ratio range 1: 0.80 – 1:1.

The report gives a systematic study of both blend ratios and the annealing temperatures. The amount of PCBM was varied in a fixed amount of P3HT. The start blend ratio of P3HT to PCBM was 1:0.80 and was varied by increasing the weight of PCBM by a step of 0.02 to a final ratio of 1:1.

Previous studies have also shown that an annealing process, normally by heating, is necessary to improve the performance of the blend thin films (Quist et al., 2005).

However, the optimum annealing temperature for the blend ratios is not clearly understood. There is need therefore to optimize both the blend ratio and annealing temperatures of P3HT: PCBM thin films. The objective of the study was to determine the optimal blend ratio and the corresponding optimal annealing temperature.

MATERIALS AND METHODS

The bulk powder form of pristine P3HT and PCBM (Kintec Company of China) were analyzed separately using XRD, FTIR spectroscopy, and HR-TEM microscopy. This was done to confirm the integrity of the two materials. The experiment used a Tecnai F20 HR-TEM microscope, a Perkin Elmer 1600 FTIR instrument, and the XRD instrument was a Rigaku D/MAX-RC make.

To develop thin films from the two materials, 50 mg of P3HT was measured on an analytical balance. Different weights of PCBM were then measured to give the appropriate ratios by weight of P3HT to PCBM as follows: 1:1, 1:0.98, 1:0.96, 1:0.94, 1:0.92, 1:0.90, 1:0.88, 1:0.86, 1:0.84, 1:0.82, and 1:0.80. The different weight mixtures were then dissolved in 5 ml of chloroform each and blended using a shaker for 6 min running at 2500 rpm to obtain homogeneous solutions. The dark red solutions were then spin coated in air on glass substrates at 800 rpm for 15 s to develop the thin films.

The thin films were then covered in aluminium foil to keep out light and stored in a dry place before annealing. Films prepared were subsequently annealed in air at temperatures of 100, 120, 130, 135, 140, 145, 150, 155, 160, 165 and 170°C for 30 min each. The films were then analyzed for optical absorption and transmittance for each of the temperatures using a CECIL 2000 UV-VIS spectrophotometer.

RESULTS AND DISCUSSION

The results of the experiment are divided into four main categories according to the type of analysis carried out. The categories are FTIR, HR-TEM, XRD, and UV-VIS results and analyses. Results from the FTIR spectra identified the presence of specific vibration modes and frequencies consistent with those from specific functional groups in the materials. HR-TEM images gave details of the particle shape and sizes, whereas XRD spectra sought to identify the materials by direct comparison of the pre-stored spectra in the database with those of the samples. The UV-VIS spectra helped to map the optical absorption and transmittance characteristics of the materials which included the percentage absorption and the wavelength position of peaks, and their full-wave half maxima (FWHM) or line widths.

The characteristic Fourier transform infrared spectroscopy (FTIR) spectra of pristine Poly (3-hexylthiophene-2, 5- diyl) (P3HT) and [6, 6] phenyl-C₆₁-butyric acid methyl ester (PCBM)

Both spectra of P3HT and PCBM exhibited absorption peaks characteristic of functional groups present in the respective materials. Figure 1 shows the measured FTIR

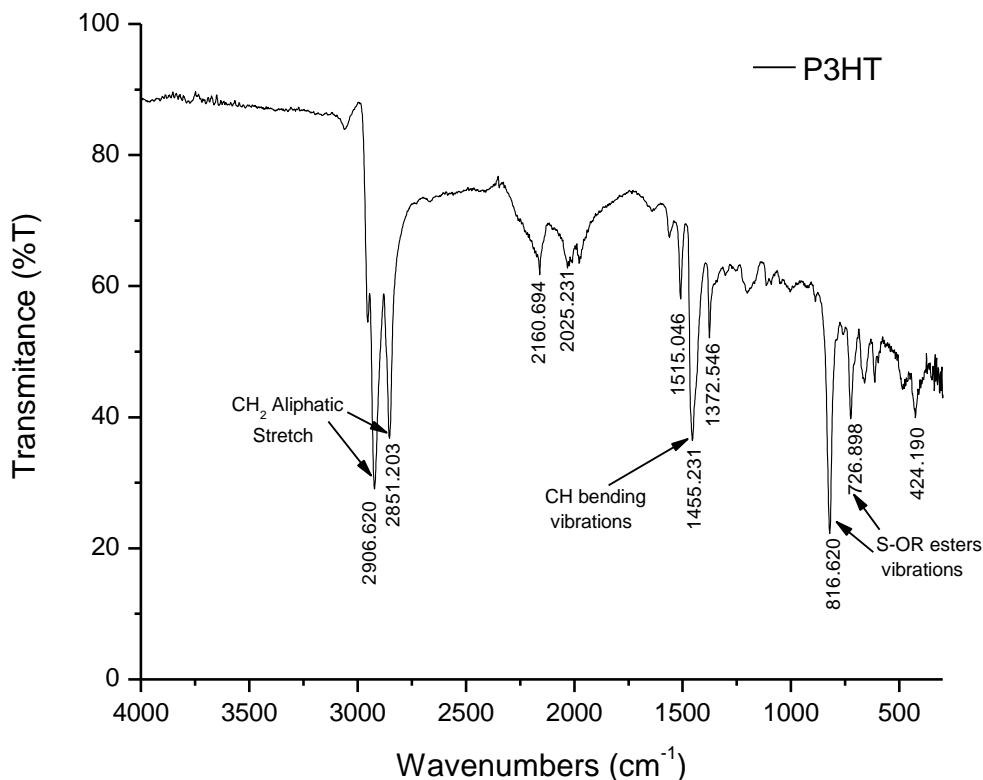


Figure 1. The measured characteristic FTIR spectrum of pristine P3HT at various frequencies.

spectrum of pristine P3HT. The presence of carbon-to-sulfur (C-S) single bond deformation vibrations was detected at 816 cm^{-1} which agrees with results from other scholars such as Shrotriya et al. (2005). The spectrum further shows the presence of carbon-to-carbon (C=C) double bonds stretching vibration at 1515 cm^{-1} . The strong stretching vibration of aliphatic (CH₂) bonds was detected at 2906 cm^{-1} . The presence of these molecules was consistent with the chemical structure of P3HT and hence confirmed the integrity of the P3HT used (Ma et al., 2005; Shrotriya et al., 2005).

Figure 2 shows the measured FTIR spectrum of pristine PCBM. It reveals a strong presence of carbon-to-hydrogen (C-H) single bonds bending and puckering at 692 cm^{-1} . The spectrum also shows another strong presence of carbon-to-oxygen (C=O) double bonds stretching at 1732 cm^{-1} frequency. The CH₂ bending was detected at 1424 cm^{-1} whilst oxygen-to-carbon (O-C) single bond vibrations were detected at 1147 cm^{-1} . The vibration position of these peaks was consistent with that of PCBM (Ma et al., 2005; Shrotriya et al., 2005).

The characteristic high resolution transmission electron microscopy (HR-TEM) images of pristine [6, 6] phenyl-C₆₁-butyric acid methyl ester (PCBM)

Figure 3 shows the HR-TEM images of PCBM at various

resolutions. Images for P3HT could not be obtained due to its poor solubility in ethanol. Images in Figure 3a and b at 5 and 10 nm resolutions, respectively, show the presence of porous fabric like sheets, which is an organic characteristic feature of the material. The image in Figure 3c at 100 nm resolution depicts particles organized in form of plates resting on top of each other and having an average thickness of about 80 nm. The image in Figure 3d at 200 nm resolution gives a side view of one of the particles in Figure 3c and reveals an irregularly fragmented plate having an average length of 600 nm. The images give evidence that when PCBM is dissolved in organic solvents like ethanol it is broken down into nano-plates which possibly rejoins upon crystallization.

The characteristic x-ray diffraction (XRD) spectra of pristine [6, 6] phenyl-C₆₁-butyric acid methyl ester (PCBM) and Poly (3-hexylthiophene-2, 5- diyl) (P3HT)

Typical measured XRD spectra of P3HT and PCBM are shown in Figure 4. The highest and dominant XRD intensity peak of P3HT powder was located at about $\theta = 12^\circ$ whilst that of PCBM was at $\theta = 10^\circ$.

The crystallite size determined from the dominant peaks was 98 nm for P3HT and 77 nm for PCBM. This showed a good agreement with the PCBM HR-TEM

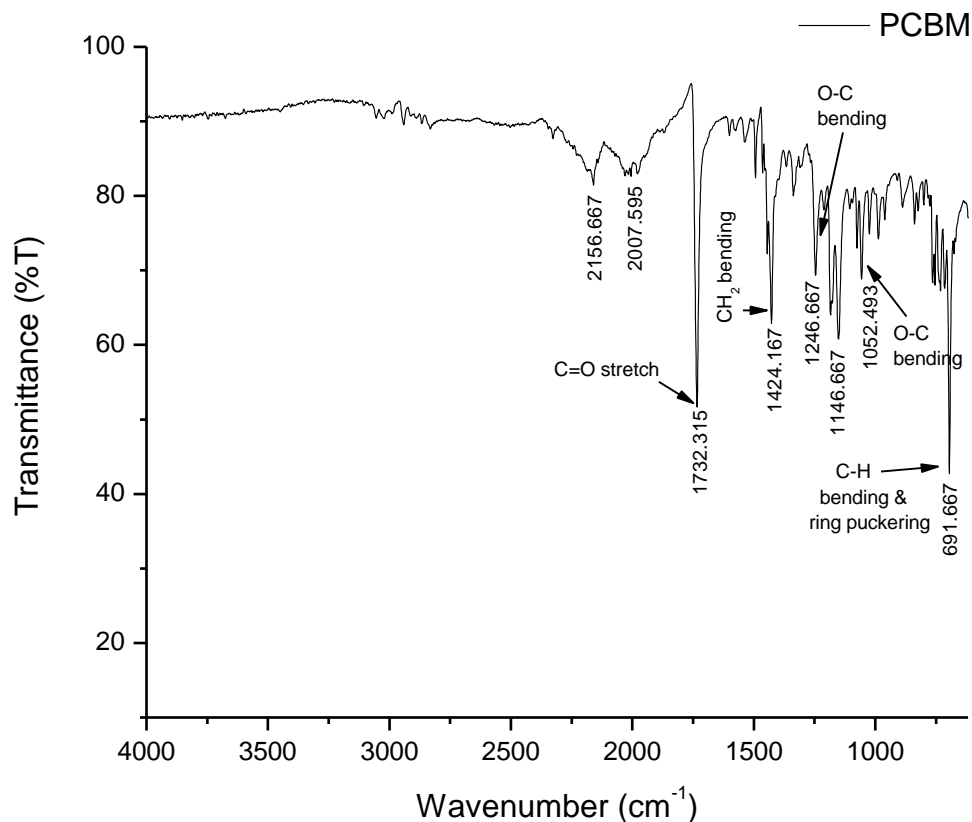


Figure 2. The measured FTIR spectrum of pristine PCBM at various frequencies.

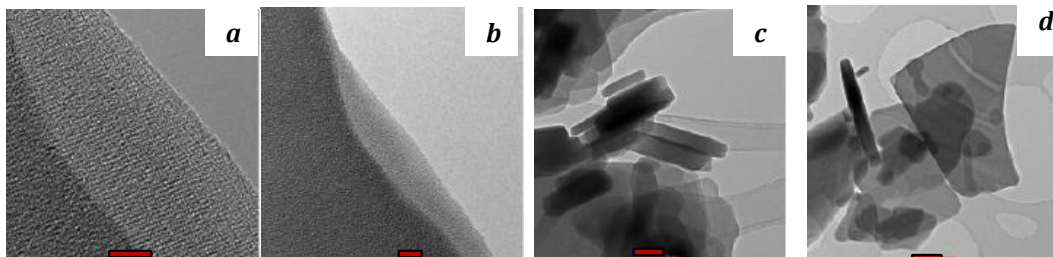


Figure 3. The measured HR-TEM images of PCBM, with **a** at 5 nm, **b** at 10 nm, **c** at 100 nm and **d** at 200 nm resolutions.

images crystallite thickness at 80 nm.

The characteristic Ultraviolet-visible spectroscopy (UV-VIS) spectra of Poly (3-hexylthiophene-2, 5- diyl) (P3HT)/ [6, 6] phenyl-C₆₁-butyric acid methyl ester (PCBM) thin films

The spectra for the as-deposited thin films of both pristine P3HT and PCBM are shown in Figure 5. P3HT shows high absorption in the visible region with a broad peak centered at about 550 nm wavelength. PCBM exhibits

general poor optical absorbance of less than 40% in the wavelength range 350 to 1100 nm with a small rise in absorption in form of a blue hump at 335 nm wavelengths and a sharp rise in regions beyond 335 nm. P3HT exhibits a red shoulder at 620 nm wavelength which is attributed to interplane interaction in the matrix of the conjugated polymer (Kim et al., 2006).

A comparison of the absorption of as-cast thin films of P3HT and some selected blends is given in Figure 6. In the visible light region, the absorption range of the blends is observed to lie between that of P3HT and PCBM, with the PCBM concentration of 1.00 having the highest peak

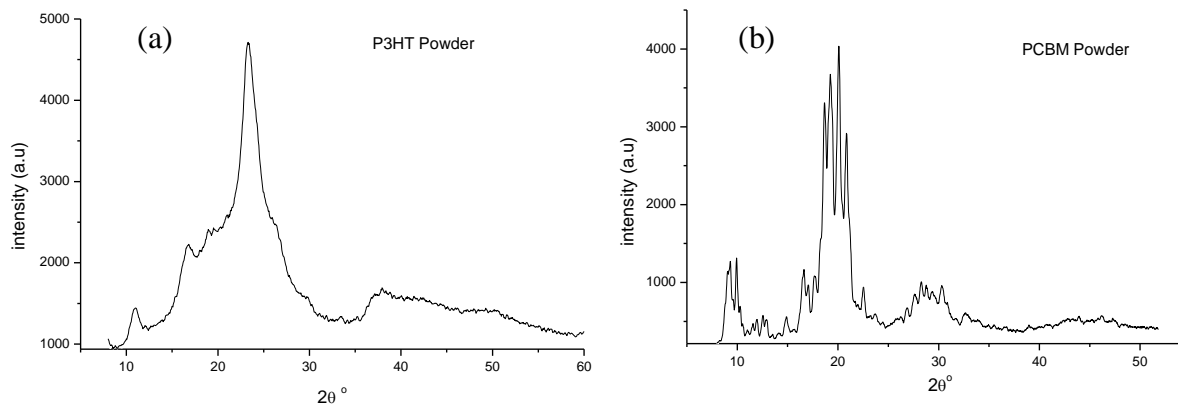


Figure 4. Measured XRD spectra of bulk (a) P3HT and (b) PCBM powders at different diffraction angles.

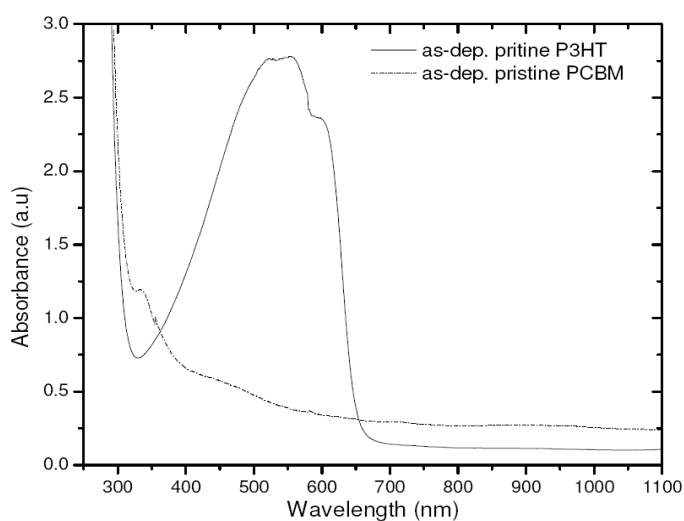


Figure 5. Graph of optical absorbance of as-deposited pristine P3HT and PCBM thin films.

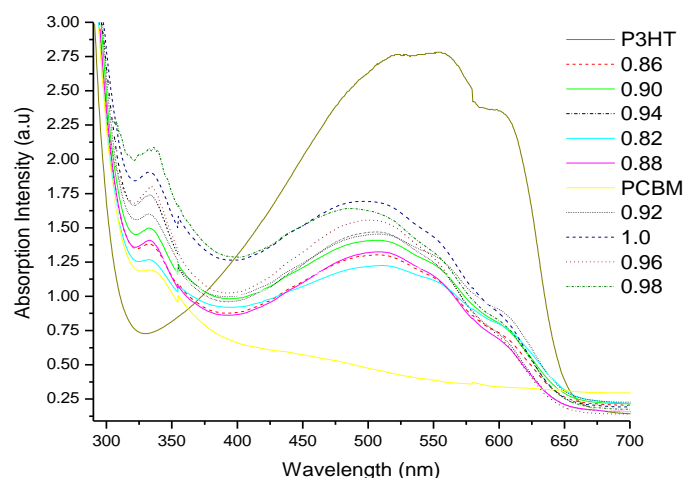


Figure 6. Optical absorbance of as-cast P3HT, PCBM and selected blend ratios showing PCBM concentrations.

while 0.80 having the lowest. Previous studies have shown that thin films with same blend ratio but varying thickness are characterized by same peak wavelength but different absorption intensities (Zeng et al., 2010). Figure 6 shows overlapping curves, a clear indication that the films are of differing blend ratios.

One observable feature in the curves of the thin films is a blue shift in peak position in comparison to that of P3HT. While the shoulder of P3HT at 600 nm wavelength is observed to maintain the same position in the blend ratios, the peaks of the blends are at varying positions from each other as well as from that of P3HT. Figure 7 shows the trend of the blue shift for peaks with varying PCBM concentration. The blue shift increases with the increase in PCBM concentration.

The blue shift is also accompanied by a general rise in absorption intensity with increase in PCBM concentration. Figure 8 shows the characteristic rise in absorption intensity that accompanies the blue shift. A similar behavior was observed in the PCBM hump at 335 nm wavelength. The intensity in the hump increased with PCBM concentration. Figure 9 shows the characteristic behavior of the PCBM hump at 335 nm in the blend films. It was observed that the hump maintained the same wavelength position despite varying in intensity, which is not the same behavior with the P3HT peaks.

To establish the blend ratio that is the best absorber, the area under the curve of the various thin films were calculated. The area under the graph of absorbance represents the total absorbance or amplitude for the given curve. For the thin films studied, the total absorbance was observed to increase linearly with the increase in PCBM concentration. Figure 10 shows the characteristic graph from the area-under-graph of the various thin film curves. The graph shows that the area increases with increase in PCBM concentration. From this graph, we are able to conclude that, within the range of the blend ratios under discussion, the 1:1 ratio is the best absorber and the least being that of 1:0.80 ratio.

The study also observed that the transmittance of

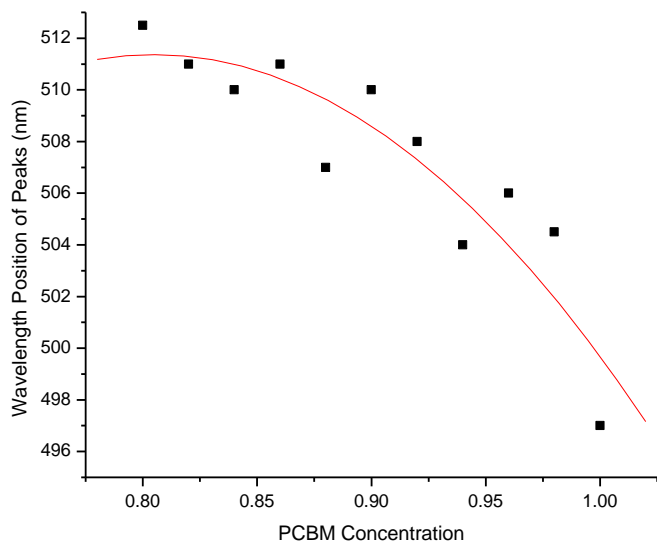


Figure 7. Blue shift in peaks with increase in PCBM concentration.

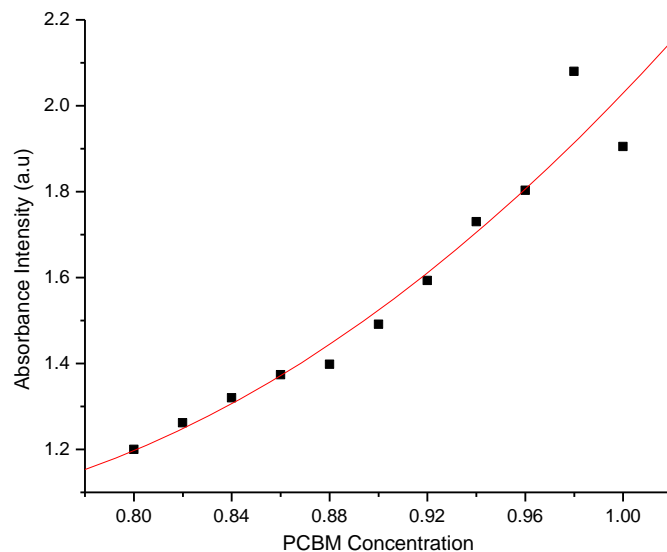


Figure 9. Intensity of PCBM hump at 335 nm wavelength on the blends.

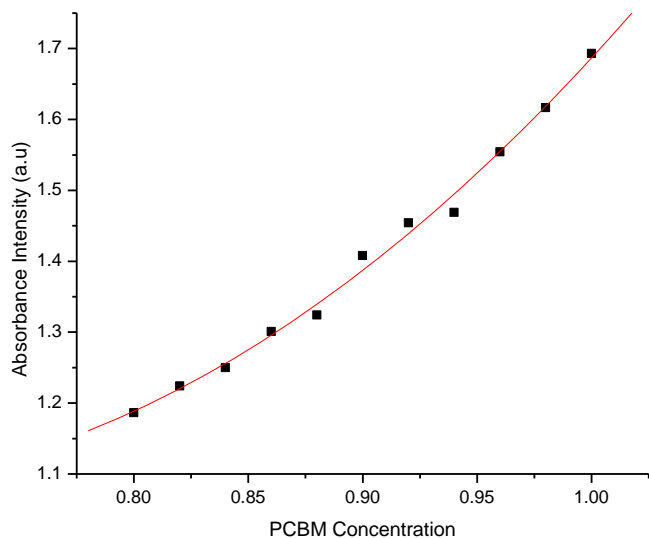


Figure 8. Characteristic rise in absorption intensity accompanying the blue shift in the P3HT/PCBM thin films

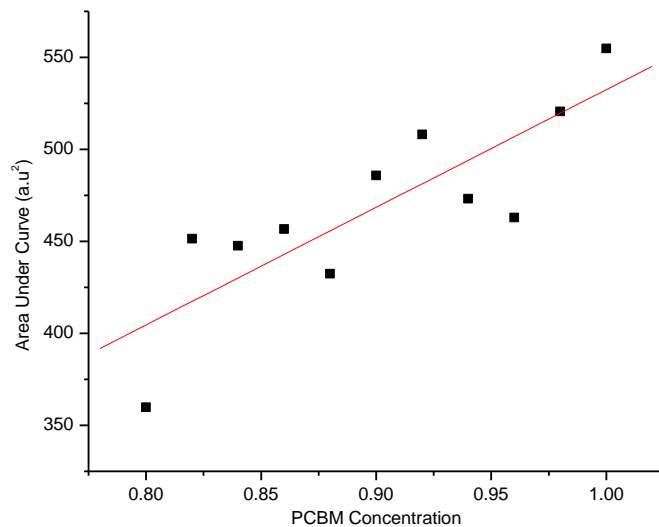


Figure 10. A plot of amplitude of the curves of P3HT/PCBM thin Films.

by the P3HT thin film. Such surface reflectance is generally undesirable for thin films as it reduces the performance of photo-devices such as solar diode and cells (Usami, 2000; Koster, 2007). The surface reflectance is however eliminated upon thermal annealing.

To fully appreciate the role of thermal annealing in the performance of these thin films, it is important to understand that when P3HT is dissolved in solvents such as chloroform, both long polymer chains which consists of co-polymer thiophene rings, and the interplane stacking supported by the alkyl side chains are broken,

P3HT between 500 and 600 nm wavelengths is largely negligible. This implies the surface reflectance is responsible for the large amount of energy not absorbed but readily re-crystallizes upon evaporation of the solvent (Woehrlé and Meissner, 1991; Kim et al., 2006; Zhao et al., 1995). The addition of PCBM molecules to dissolved P3HT matrix however inhibits the re-stacking and re-formation of long chains in the as-deposited thin films matrix of the latter. This is because PCBM crystallizes more readily and faster compared to P3HT and forms homogeneous crystals when spin cast at room temperature. This in turn inhibits P3HT's crystallization.

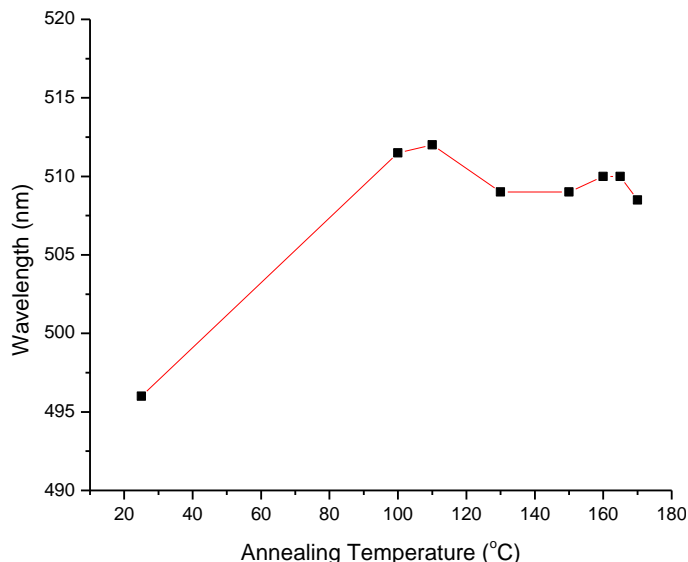


Figure 11. Red shift in 1:1 blend ratio with annealing. The graph is a plot of the peak positions at each annealing temperature.

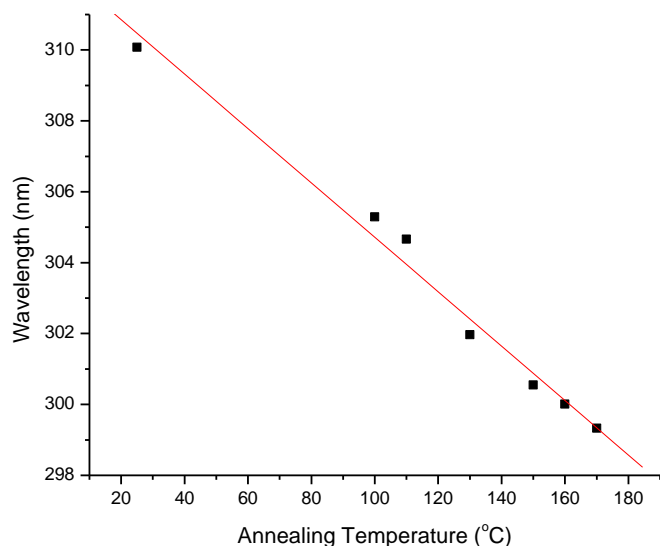


Figure 12. Blue shift in pristine PCBM with annealing temperature.

However, upon annealing PCBM segregates and forms disjointed clusters of islands as its crystals begin to breakup. XRD results reported by other scholars have shown that PCBM crystallinity is largely absent in annealed 1:1 blends whereas in as-cast films it is present (Beal et al., 2010). Hence annealing of pure PCBM films may be undesirable as it destroys crystals in the film. In blend materials however, when annealed, the segregated PCBM small molecules diffuse into the P3HT matrix allowing the latter to re-organize itself into stacks and long chains as a result of the increase in mean free volume. Raman microscopy results have previously

shown that upon annealing the relative position of P3HT remains largely the same while that of PCBM changes, a clear indication that PCBM aggregates and diffuses into P3HT matrix during the annealing process (Klimov et al., 2006; Marchaut and Foot, 1997; Hugger et al., 2003; Zhao et al., 2009).

This study indicates that crystallization of P3HT in the blends upon annealing improves the absorption of the films and causes a red shift to occur in the spectra of the blends. This effect is clearly observed in Figure 11 and shows that a major red shift occurs at temperatures of as low as 100°C and remains almost constant thereafter. On the other hand, although PCBM crystallizes easily at low temperatures, an annealing process has been observed to cause a blue shift in pristine PCBM as can be observed from Figure 12.

Since PCBM more readily crystallizes at low temperatures compared to P3HT, it follows that the influence of PCBM in the blends is more prominent at low annealing temperatures and is suppressed at higher values. This effect has been observed from Figures 6 where the as-cast pristine P3HT exhibit a well pronounced red shoulder at 620 nm wavelengths which is attributed to the inter-plane interaction in the matrix of P3HT. This shoulder is however less pronounced in the as-cast blends, owing to the influence of PCBM.

In addition, increasing PCBM content in the blend leads to an increase in the glass transition temperature of the blend as a whole. PCBM has a glass transition temperature of 131.2°C compared to that of P3HT at 12.1°C. On the other hand, a reduction in the glass transition temperature of the blend is expected with increasing P3HT content. The shift in these two key transition temperatures as a function of blend composition underscores the importance of determining the optimal thermal annealing temperatures for a given blend ratio (Woehrle and Meissner, 1991; Zhao et al., 1995; Mattis et al., 2003; Verploegen et al., 2010; Taghavi and Hirata, 2010). This, to a large extent, guides the annealing process of the thin films.

The trend observed upon annealing in the absorption spectra of the blends with a red shift is attributed to the improved crystallization in P3HT and molecular diffusion of PCBM into the stacking of P3HT chains.

Figure 13 depicts changes that occur upon thermal annealing in pristine PCBM while Figure 14 depicts the changes in P3HT.

From Figures 15 it is observed that upon annealing, the absorption spectrum of the P3HT:PCBM composite undergoes a strong modification, whereas in the pure components of Figure 13 and 14 it remains largely unchanged. The thermal annealing process therefore allows for modification of the morphology of the blends causing phase changes.

From Figure 16 it is seen that each blend ratio of P3HT:PCBM has its own optimum annealing temperature just as each blend ratio has a different optimum absorbance value (Figure 8). This can be explained from the

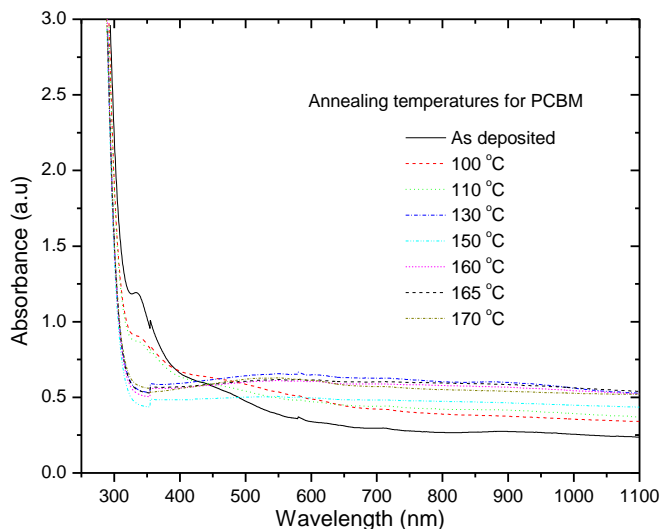


Figure 13. Measured changes upon thermal annealing in PCBM.

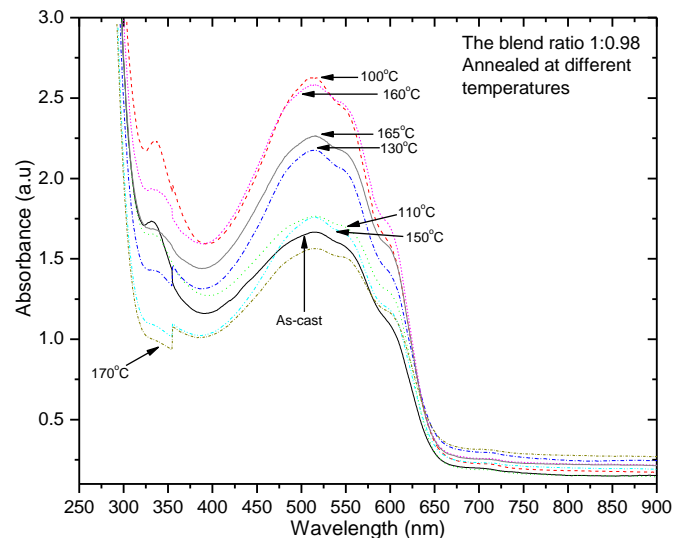


Figure 15. The absorption spectrum of 1:0.98 annealed at different temperatures.

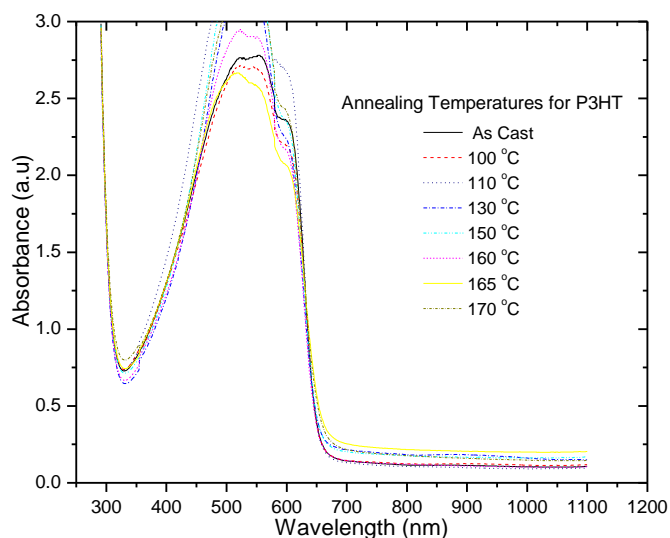


Figure 14. Measured changes upon thermal annealing in P3HT at different temperatures.

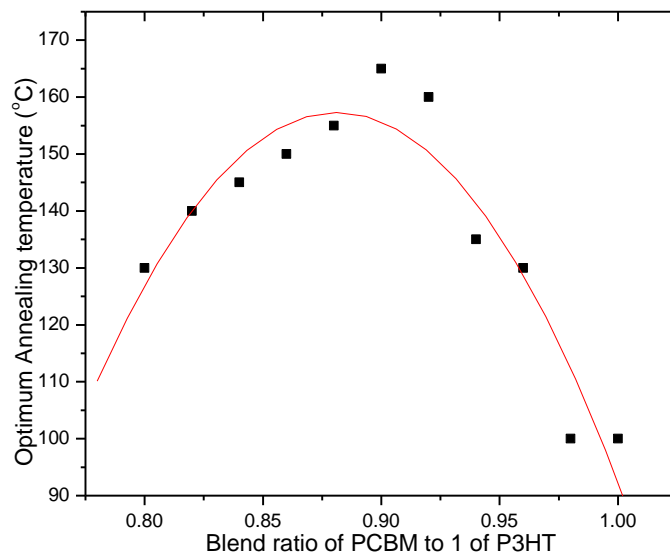


Figure 16. The optimum annealing temperatures for different blend ratios.

understanding that each blend ratio has a unique glass transition and melting temperatures. Additionally, Figure 16 shows that optimum annealing temperatures increase with the increase in PCBM concentration until at 0.90 at which it begins to fall. Furthermore, the highest optimum annealing temperature for these organic blends was found to be at about 165°C corresponding to the 1:0.90 ratio.

Conclusion

The blend ratio of P3HT:PCBM was characterized and optimized within the range of 1:0.8 to 1:1 at an increment

interval of 0.02 for PCBM as P3HT was kept constant. Each blend ratio was found to have its own best annealing temperature. On the other hand, the annealing process was found to improve the absorption performance of the blend ratios.

It was found that a blue shift in absorption peaks increased with the increase in PCBM concentration. The annealing process was however observed to cause a red shift in the individual blends. On the other hand an analysis on the area-under-curve showed that the areas for the different curves were linear and increased with PCBM concentration. The highest absorption among the

blends was observed from that of 1:1 blend at an annealing temperature of 100°C. This was followed by the 1:0.98 blend at 100°C annealing temperature. Therefore 1:1 is considered as the optimal blend ratio with an optimum annealing temperature of 100°C for 30 min duration. However, all blend ratios showed a common high absorption at 130°C for duration of 30 min annealing process. A correlation between the absorption and annealing temperature for different blend ratios was clearly observed.

The addition of PCBM to P3HT was found to inhibit the crystallization of the latter and caused a blue shift in the spectrum. An annealing process was found to increase the absorption which is understood to result from the crystallization of P3HT and the segregation of PCBM in the composite.

Future work can focus on determining the glass transition temperature of the different blends, its influence on the optimal absorbance, and annealing temperatures which may provide insight as to why 1:1 is the optimum and not the other ratios.

ACKNOWLEDGEMENTS

The authors gratitude go to the Departments of Physics and Chemistry at the University of Zambia for the initial experiments, the Materials Research Group (MRG) of iThemba LABS of Cape Town in South Africa for the research facilities, the African Laser Centre (ALC) and Nanosciences African Network (NANOAFNET) for the financial support which enabled the successful completion of this research. G. Kalonga is also thankful to the International Science Programme of Uppsala University in Sweden for sponsoring most of his M.Sc. degree program. The authors acknowledge the encouragement and support rendered by research scholars throughout the period of this research.

REFERENCES

- Adam D, Closs F, Frey T, Funhoff D, Haarer D, Ringsdorf H, Schuhmacher P, Siemensmeyer K (1993). Transient photoconductivity in a discotic liquid crystal. *Phys. Rev. Lett.* 70(4):457-460.
- Beal RM, Stavrinadis A, Warner JH, Smith JM, Assender HE, Watt AAR (2010). The molecular structure of polymer-fullerene composite solar cells and its influence on device performance. *Macromolecules* 43(5):2343-2348.
- Brabec CJ, Sariciftci NS, Hummelen JC (2001). Plastic solar cells. *Adv. Funct. Mater.* 11(1):15-26.
- Camaioni N, Ridolfi G, Miceli GC, Possamai G, Maggini M (2002). The effect of a mild thermal treatment on the performance of poly(3-alkylthiophene)/fullerene solar cells. *Adv. Mater.* 14(23):1735-1738.
- Chen LM, Hong Z, Li G, Yang Y (2009). Recent progress in polymer solar cells: manipulation of polymer-fullerene morphology and the formation of efficient inverted polymer solar cells. *Adv. Mater.* 21(14-15):1434-1449.
- Chirvase D, Parisi JC, Hummelen JM, Dyakonov V (2004). Influence of nanomorphology on the photovoltaic action of polymer-fullerene composites. *Nanotechnol.* 15(9):1317-1323.
- Dennler G, Scharber MC, Brabec CJ (2009). Polymer-fullerene bulk-heterojunction solar cells. *Adv. Mater.*, 21(13):1323-1338.
- Dunlap DH, Parris PE, Kenkre VM (1996). Charge-dipole model for the universal field dependence of mobilities in molecularly doped polymers. *Phys. Rev. Lett.* 77(3):542-545.
- Friend RH, Denton GJ, Halls JJM, Harrison NT, Holmes AB, Kohler A, Lux A, Moratti SC, Pichler K, Tessler N, Towns K (1997). Electronic processes of conjugated polymers in semiconductor device structures. *Synth.Met.* 84(1-3):463-470.
- Gartstein YN, Conwel EM (1995). High-field hopping mobility in molecular systems with spatially correlated energetic disorder. *Chem. Phys. Lett.* 245(4-5):351-358.
- Green MA (1982). *Solar cells: operating principles, technology and system applications.* Prentice-Hall, Englewood Cliffs, New Jersey.
- Hoppe H, Drees M, Schwinger W, Schaffler F, Sariciftci NS (2005). Nano-crystalline fullerene phases in polymer/fullerene bulk-heterojunction solar cells: A transmission electron microscopy study. *Synth. Met.* 152(1-3):117-120.
- Hugger S, Thomann R, Heizel T, Albiecht TT (2003). Semicrystalline morphology in thin films of poly(3-hexylthiophene). *Colloid Polym. Sci.* 282(8):932-938.
- Kim Y, Cook S, Tuladhar SM, Choulis SA, Nelson J, Durrant JR, Bradley DDC, Giles M, McCulloch I, Chang-Sik HA, Ree M (2006). A strong regioregularity effect in self-organizing conjugated polymer films and high-efficiency polythiophene:fullerene solar cells. *Nature Mater.* 5(5):197-203.
- Klimov E, Li W, Yang X, Hoffmann GG, Loos J (2006). Scanning near-field and confocal raman microscopic investigation of P3HT-PCBM systems for solar cell applications. *Macromolecules* 39:4493-4496.
- Koster LJA (2007). *Device physics of donor-acceptor/blend solar cells,* PhD Thesis, University of Groningen, The Netherlands.
- Lane PA, Rostalski J, Giebeler C, Martin SJ, Bradley DDC, Meissner D (2000). Electroabsorption studies of phthalocyanine/perylene solar cells. *Solar Energy Mater. Solar Cells* 63(1):3-13.
- Ma W, Yang C, Gong X, Lee K, Heeger AJ (2005). Thermally stable, efficient polymer solar cells with nanoscale control of the interpenetrating network morphology. *Adv. Funct. Mater.* 15(10):1617-1622.
- Marchaut S, Foot PJS (1997). Annealing behaviour of conductive poly(3-hexylthiophene) films. *Polymer* 38(7):1749-1751.
- Mattis BA, Chang PC, Subramanian V (2003). Effect of thermal cycling on performance of poly(3-hexylthiophene) transistors. *Mater. Res. Soc. Symp. Proc. MRS Spring Meeting, Symp. L, 771:369-374.*
- Muhlbacher D, Scharber M, Morana M, Zhu Z, Waller D, Gaudiana R, Brabec C (2006). High photovoltaic performance of a low-bandgap polymer. *Adv. Mater.* 18(21):2884-2889.
- Nguyen LH, Hoppe H, Erb T, Gunes S, Gobsch G, Sariciftci NS (2007). Effects of annealing on the nanomorphology and performance of poly(alkylthiophene): Fullerene bulk-heterojunction solar cells. *Adv. Funct. Mater.* 17(7):1071-1078.
- Quist PAC, Savenije TJ, Koetse MM, Veenstra SC, Kroon JM, Siebbeles LDA (2005). The effect of annealing on the charge-carrier dynamics in a polymer/polymer bulk heterojunction for photovoltaic applications. *Adv. Funct. Mater.* 15(3):469-474.
- Shaheen SE, Brabec CJ, Sariciftci NS, Hummelen JC (2001). 2.5% efficient organic plastic solar cells. *Appl. Phys. Lett.* 78(6):841-843.
- Shockley W, Queisser HJ (1961). Detailed balance limit of efficiency of P N junction solar cells. *J. Appl. Phys.* 32(3):510-519.
- Shrotriya V, Ouyang J, Tseng RJ, Li G, Yang Y (2005). Absorption spectra modification in poly(3-hexylthiophene): Methanofullerene blend thin films. *Chem. Phys. Lett.* 411(1-3):138-143.
- Sze SM (1981). *Physics of semiconductor devices,* 2nd Edition, Wiley, New York.
- Taghavi HV, Hirata A (2010). Deposition of unhydrogenated amorphous carbon films by sublimation of C60 fullerene in electron beam excited plasma. *Mater. Lett.* 64(1):83-85.
- Usami A (2000). Theoretical simulations of optical confinement in dye-sensitized nanocrystalline solar cells. *Solar Energy Mater. Solar Cells* 64(1):73-83.
- Verploegen E, Mondal R, Bettinger CJ, Sok S, Toney MF, Bao Z (2010). Effects of thermal annealing upon the morphology of polymer-fullerene blends. *Adv. Funct. Mater.* 20(20):3519-3529.

Woehrle D, Meissner D (1991). Organic solar cells. *Adv. Mater.* 3(3):129–138.

Zeng L, Tang CW, Chen SH (2010). Effects of active layer thickness and thermal annealing on polythiophene: Fullerene bulk heterojunction photovoltaic devices. *Appl. Phys. Lett.* 97:5. doi:10.1063/1.3474654.

Zhao J, Swinnen A, van Assche G, Manca J, Vanderzande D, van Mele B (2009). Phase diagram of P3HT/PCBM blends and its implication for the stability of morphology. *J. Phys. Chem. B* 113(6):1587-1591.

Zhao Y, Yuan G, Roche P (1995). A calorimetric study of the phase transitions in poly(3-hexylthiophene). *Polymer* 36(11):2211-2214.